GA–A23409

EXPERIMENTS AND COMPUTATIONAL MODELING FOCUSED ON DIVERTOR AND SOL OPTIMIZATION FOR ADVANCED TOKAMAK OPERATION ON DIII–D

by
S.L. ALLEN, J.A. BOEDO, A.S. BOZEK, N.H. BROOKS, T.N. CARLSTROM, T.A. CASPER, R.J. COLCHIN, T.E. EVANS, M.E. FENSTERMACHER, M.E. FRIEND, R.C. ISLER, R. JAYAKUMAR, C.J. LASNIER, A.W. LEONARD, M.A. MAHDAVI, R. MAINGI, G.R. McKEE, R.A. MOYER, M. MURAKAMI, T.H. OSBORNE, R.C. O'NEILL, T.W. PETRIE, G.D. PORTER, A.T. RAMSEY, M.J. SCHAFFER, P.G. STANGEBY, R.D. STAMBAUGH, M.R. WADE, J.G. WATKINS, W.P. WEST, D.G. WHYTE, and N.S. WOLF

JUNE 2000

DISCLAIMER

GA–A23409

EXPERIMENTS AND COMPUTATIONAL MODELING FOCUSED ON DIVERTOR AND SOL OPTIMIZATION FOR ADVANCED TOKAMAK OPERATION ON DIII–D

by
S.L. ALLEN,* J.A. BOEDO,† A.S. BOZEK, N.H. BROOKS, T.N. CARLSTROM, T.A. CASPER,* R.J. COLCHIN,‡ T.E. EVANS, M.E. FENSTERMACHER,* M.E. FRIEND, R.C. ISLER,‡ R. JAYAKUMAR,* C.J. LASNIER,* A.W. LEONARD, M.A. MAHDAVI, R. MAINGI,# G.R. McKEE,△ R.A. MOYER,† M. MURAKAMI,‡ T.H. OSBORNE, R.C. O'NEILL, T.W. PETRIE, G.D. PORTER,* A.T. RAMSEY,* M.J. SCHAFFER, P.G. STANGEBY,§ R.D. STAMBAUGH, M.R. WADE,‡ J.G. WATKINS,∞ W.P. WEST, D.G. WHYTE,† and N.S. WOLF*

This is a preprint of a paper presented at the 14th International Conf. on Plasma Surface Interactions in Controlled Fusion Devices, May 22–26, 2000 in Rosenheim, Germany and to be published iin *J. Nucl. Mater.*

*Lawrence Livermore National Laboratory, Livermore, California.
†University of California, San Diego, La Jolla, California.
‡Oak Ridge National Laboratory, Oak Ridge, Tennessee.
#Princeton Plasma Physics Laboratory, Princeton, New Jersey.
△University of Wisconsin, Madison, Wisconsin.
§University of Toronto Institute for Aerospace Studies, Toronto, Canada.
∞Sandia National Laboratories, Albuquerque, New Mexico.

Work supported by
the U.S. Department of Energy under Contract Nos. DE-AC03-99ER54463, W-7405-ENG-48, DE-AC05-00OR22725, DE-AC02-76CH03073, DE-AC04-94AL85000, and Grant Nos. DE-FG03-95ER54294 and DE-FG02-92ER54139

GA PROJECT 30033
JUNE 2000

ABSTRACT

We present results from DIII–D experiments and modeling focused on the divertor issues of an "Advanced Tokamak" (AT). Operation at high plasma pressure β with good energy confinement H requires core and divertor plasma shaping and current profile J(r) control with ECH current drive. Transport modeling indicates that the available DIII–D ECH power determines a density and temperature regime for sustained DIII–D AT experiments. We demonstrate that a high-δ, unbalanced double null divertor with cryopumping (D-2000) is a flexible AT divertor. Impurity levels in AT experiments have been reduced by careful alignment of the divertor tiles; this, in turn has changed the time evolution of the core J(r) profiles. New physics has been observed near the X-point and private flux regions, including flow reversal and recombination, that is important in understanding and controlling the flows and thereby the radiation in the divertor region, which reduces the divertor heat flux.

1. INTRODUCTION

For the past decade, tokamak divertor research has been focused on the control of power and particles. Experiments have shown that the tokamak power exhaust is concentrated in a small area, so impurities radiating in the divertor have been used to disperse the exhaust and lower the heat flux to the walls. Active particle exhaust with divertor cryopumping is used for the control of density and impurities in the plasma core. These results formed the basis for the ITER divertor design [1] and a recent U.S. national workshop [2] also concluded that we have a reasonable scientific basis for a conventional long-pulse divertor solution at high density (i.e., a collisional edge plasma). There are still concerns, however, about *simultaneously* handling ELMs and off-normal events like disruptions, along with the tritium inventory. Another challenge is to find self-consistent operating modes for other configurations, including optimized or "Advanced Tokamaks" (AT) and alternate magnetic geometries [2].

In the radiative or dispersive divertor, deuterium puffing is used to increase the divertor radiation which in turn forms a low electron temperature recombining plasma near the plate [3,4]. This "detached" divertor plasma reduces the peak heat and particle fluxes to the divertor plate. Both deuterium and helium control can be achieved in these "Partially Detached Divertor" (PDD) discharges [5–7] since, even though there is strong detachment near the divertor strike point, the particle flux away from the strike point (i.e. outboard towards the cryopump) is sufficient for particle exhaust. Currently, the PDD regime is obtained at core densities of about 0.6 to 1.4 times the Greenwald density $n_e/n_{gw} \equiv n_e/I_p\ (\pi a^2)$. In DIII–D, the energy confinement time H-factor, $H = (\tau_E/\tau_{ITER\text{-}89P})$ is ~1.8–2.0 for PDD operation, showing good H–mode confinement even above the Greenwald density. We have found that divertor pumping and/or maintaining sufficient edge pedestal temperature is important for maintaining good confinement at high density [8].

Impurity control has also been demonstrated in the PDD regime, with a core $Z_{eff} < 1.8$ routinely obtained in ELMing H–mode with carbon walls. Strong D_2 midplane gas puffing (~300 Torr ℓ s^{-1}) coupled with equal exhaust by cryopumping {so-called "puff and pump" (P&P) operation [9]} to maintain a constant density also reduces the core impurity content and reduces the large pulsed heat and particle flux of edge localized modes (ELMs) on the divertor plate. Other impurities have been introduced into the divertor during P&P to enhance the radiation in the divertor and the mantle around the core. In these experiments, both the intrinsic carbon and the impurity (neon, argon) radiation in the divertor increase, and there is an increased concentration of the impurity in the divertor. Erosion studies with the DiMES probe have shown that there is very little net surface erosion of the graphite divertor plates in PDD plasmas [10], in

contrast to the erosion measured in attached ELMing H–mode plasmas. Detailed surface studies indicate that over 30 boronization wall conditioning cycles and 10^5 seconds of plasma exposure during the last seven years in DIII–D have reduced the carbon chemical erosion yield by nearly 20 times, with a reduction in the carbon sputtering source by over a factor of four. The fact that the average measured core carbon content has not changed appreciably during this period points either to the importance of impurity transport in the divertor and scrape-off-layer (SOL), or to impurity sources other than the divertor. UEDGE modeling shows that radial transport in the far SOL above the X-point is important in determining the core impurity content, indicating the importance of flow and drifts in the divertor in determining the impurity behavior [11,12].

In concert with these significant advances in divertor science, a parallel effort in tokamak confinement and stability improvement has developed an "Advanced Tokamak" concept that relies on control of the plasma cross-sectional shape and the internal profiles [13-15]. If the present projections are realized, appreciable reductions in the size and cost of an AT reactor are possible [16]. We presently envision a shaped, compact plasma operating: (a) at high confinement with $H > 2$ and approaching 3, (b) with high normalized beta [$\beta_N = \beta/(I/aB)$ where I is the plasma current, a is the minor radius, and B is the magnetic field] greater than 3 and approaching 5, and (c) with little or no inductive current drive. Electron cyclotron current drive (ECCD), which can be easily "steered" and applied to a particular region of the profile, is the main current profile control tool. A DIII–D AT scenario has been developed with transport modeling; the parameters that are most important to the divertor design are the core density (0.4 to 0.6 of the Greenwald density as the amount of driven ECCD depends on n_e and T_e), low impurity concentration ($Z_{eff} < 2$), and the high-δ (triangularity) plasma shape. In this paper, we will examine the DIII-D scenario (Sec. 2), present results for the new AT divertor (Sec. 3), and then discuss new techniques for heat flux control (Sec. 4).

2. THE DIII–D AT SCENARIOS DETERMINE DIVERTOR REQUIREMENTS

Experiments and computational modeling have shown that plasma shaping (elongation κ, and triangularity δ) is a key ingredient in AT operation, as it allows operation at higher β_N. The electron pressure in the edge pedestal, necessary for good H-mode confinement, also increases with triangularity. Theory predicts that a double-null (DN) divertor has improved MHD stability. Furthermore, we have shown experimentally that the H–mode power threshold depends on several details of the divertor geometry. The power threshold increases with the distance of the X-point above the divertor floor, and increases when the direction of the ∇B drift is from the divertor to the core plasma. The up/down balance of a DN divertor plasma also changes the H–mode power threshold. We will see later in the discussion of the AT scenarios that these are valuable control tools, as the divertor particle and power exhaust can also be varied with these divertor configuration changes.

Just as these changes in the "external" magnetic geometry have been used to increase performance, optimization of the internal magnetic geometry, i.e. the shear in the q(r) (safety factor) can also improve the confinement and stability of the AT plasma. Optimized (weakly negative) central shear or OCS operation has been shown to be more favorable for long-pulse operation, and is the mode chosen for near-term exploration on DIII–D. In developing the OCS profiles, the time evolution of the radial q profile is determined by the applied (ohmic plus auxiliary) current drive and current diffusion due to the plasma resistivity. The plasma resistivity is determined by core impurity density and electron temperature. In turn, the impurity density and T_e are influenced by the core and divertor impurity sources and transport. This coupling means that the divertor and SOL conditions are important in determining the time-evolution of the q-profile, which directly determines the performance of the AT scenario.

While the sustained AT scenario requires ECCD, significant progress has been made to date with OCS operation with careful control of the neutral beam injection (NBI). Detailed time-resolved measurements of the q-profile with the Motional Stark Effect (MSE) diagnostic have shown that careful NBI timing can be used to control the q-profile and weak or negative central shear profiles have been obtained. Stabilization of the resistive wall mode (by placing the plasma close to the conducting vessel wall and by real-time feedback stabilization with external coils) and neoclassical tearing modes (with shear control) has resulted in discharges with $\beta_N > 3.5$ and $H_{89} > 2.5$ for over 2 seconds. The resulting figure of merit β_N H product is 9 for over 16 energy confinement times. The bootstrap current (driven by the pressure gradient) fraction for this discharge exceeds 50%, and the total non-inductive fraction is 75%. A plot of the $\beta_N H$ product as

a function of $\tau_{duration}/\tau_E$ for several types of DIII–D discharges are shown in Fig. 1; recent data values (shots 98965 and 98977) are highlighted. The advanced tokamak "target" region is shown by the shaded box, along with approximate values for the ARIES-RS design. Several different approaches using NBI heating current profile control are presented in the figure, including a ELM-free H–mode or VH–mode (which has so far been limited to short duration), ELMy H–mode (like shot 98965, standard scenario), and a L–mode edge. To date, we have focused on the ELMy H–mode scenario as it has shown the most promise for steady-state, high performance in experiments.

Sustained AT modes require localized non-inductive current drive with ECCD, and transport modeling with the ONETWO and CORSICA codes has been used to develop scenarios for several DIII–D gyrotron power levels. The calculated current profiles for the DIII–D OCS scenario are shown in Fig 2; the input power is ~2.3 MW. ECCD is advantageous because it provides highly localized current drive and a reasonable amount of current can be driven with modest power levels. The resonance location is set by the gyrotron frequency and the local toroidal magnetic field. ECCD is also favorable from the plasma surface interactions point of view because there is no evanescent region between the antenna and the plasma; the wave is injected into the plasma with steerable launchers that are located remotely away from the plasma. The 110 GHz gyrotrons are located away from the tokamak, and flexible waveguides couple the microwaves to the launcher.

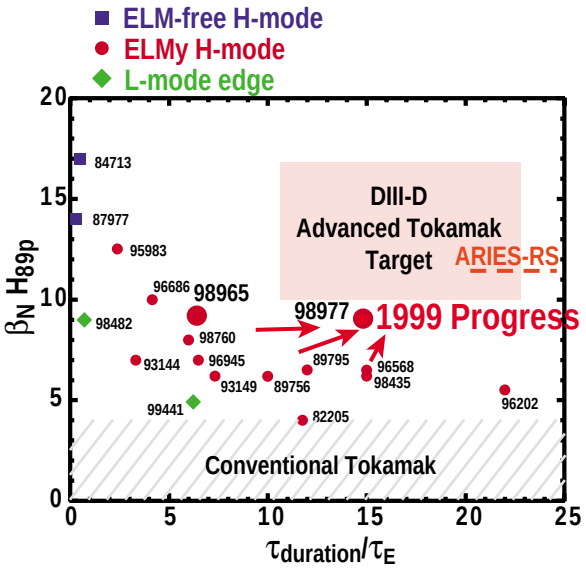

Fig. 1. A plot of the $\beta_N H$ product as a function of $\tau_{duration}/\tau_E$ for several types of DIII–D discharges with ohmic and NBI current profile control. ELM-free H–modes have good confinement but have been limited to short duration. The ELMy H–mode has achieved the best performance so far; recent discharges (98977 and 98965) are highlighted. The shaded box represents an AT target, and typical parameters for the ARIES-RS reactor design are included.

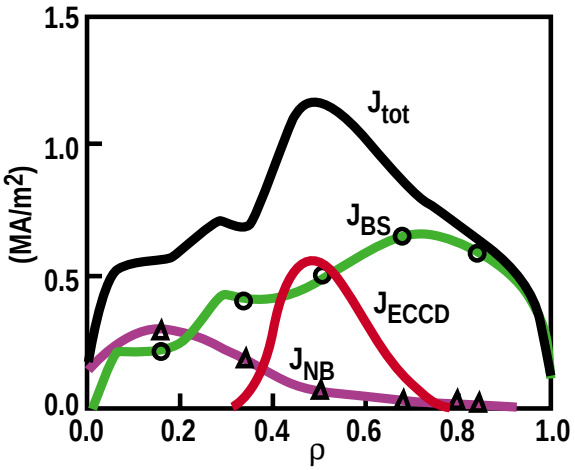

Fig. 2. Calculation of the required current profiles for a sustained ECCD AT scenario obtained from the ONETWO transport model. Note that for ECH power levels ~3 MW, the divertor must control the density in the range of 40% of the Greenwald density.

The principle requirement that ECCD in the AT scenario places on the divertor system is core density and impurity control. While the microwaves can be cutoff if the core plasma density is too high, the dependence of ECCD efficiency on density and temperature is usually a much more stringent requirement. An approximate relation for the ECCD efficiency is given by: $\eta \sim T_e/n_e^2\ (5+Z_{eff})$. This relationship, along with the available DIII–D gyrotron power and the required ECCD current, sets the core operating density. This is in the range of 0.3–0.4 of the Greenwald density for present DIII–D experiments. A set of transport calculations with the ONETWO and CORSICA transport codes have been used to study the sensitivity of the ECCD current drive to the line-average density. With an ECH input power of 2.3 MW, consistent with the available power for the year-2000 campaign, the models predict a scenario with $\beta_N \sim 4.0$ and $H_{89} \sim 2.8$ can be sustained.

3. PARTICLE AND IMPURITY CONTROL IN DIII–D AT PLASMAS WITH DIVERTOR-2000

3.1. REDUCED CORE IONIZATION WITH MORE BAFFLED DIVERTORS

The new DIII–D divertor, D-2000, is designed for high-δ plasma shapes and adds an additional helium cryopump, more baffling, and improved tile alignment at the inner strike point compared to the previous D-1998. Simplified cross sections of D-1998 (left) and D-2000 (right) are shown in Fig. 3 and a detailed cross section of D-2000 with the new diagnostics is shown in Fig. 4. The D-2000 allows flexible particle control with pumping at either the inner or outer strike points separately, or together. A private flux "dome" has been added to protect the cryopump and provide additional baffling. Although included in earlier plans, the baffle on the inner wall was not installed. This decision emphasized additional AT shape flexibility at the expense of a modest increase in divertor baffling. The tiles on the inner wall surrounding the inner strike point have been carefully contoured to the magnetic field to minimize edge heating.

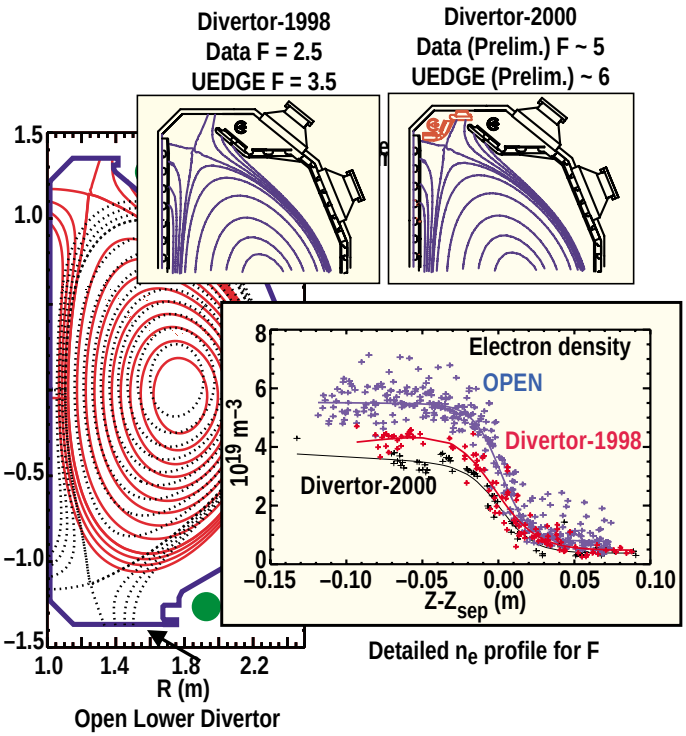

Fig. 3. A comparison of the reduction in the core ionization compared to the open (lower divertor) which is defined as F. The edge density and temperature profiles are used to determine F ~ 2.6 for D-1999 and F ~ 5 D-2000, in reasonable agreement with the UEDGE modeling.

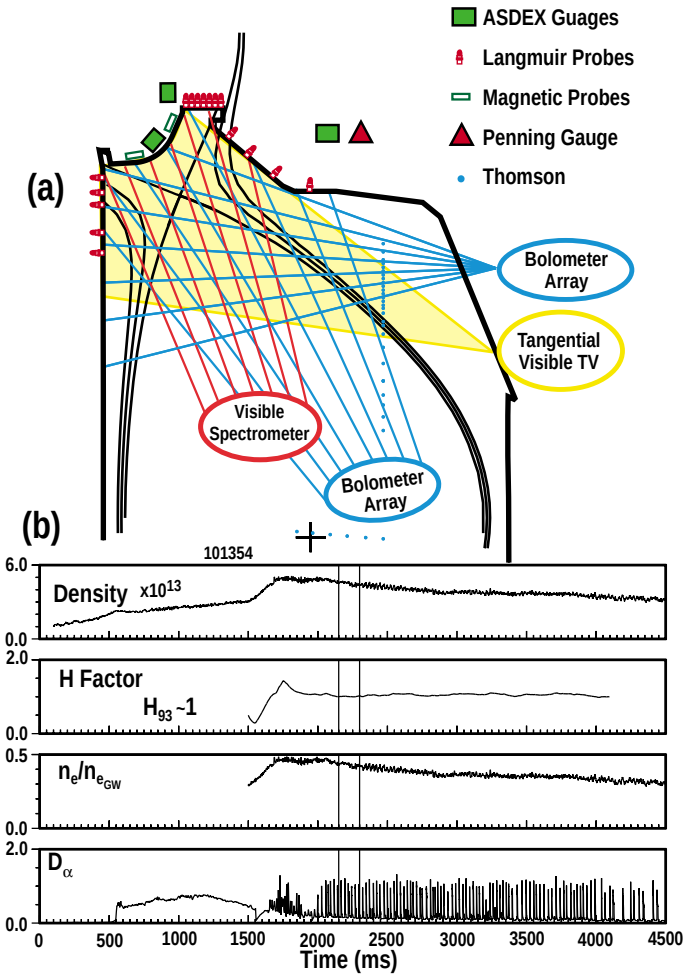

Fig. 4. Several new diagnostics have been installed with D-2000, including an array of Langmuir probes, ASDEX and Penning gauges, visible spectroscopy views, and a visible TV camera. D-2000 has been used to reduce the core electron density to 30%–40% of the Greenwald density, which is sufficient for the AT scenarios with the current ECCD power on DIII–D.

In an ongoing comparison between model predictions and experimental results, we have used the benchmarked UEDGE model of the edge plasma, along with Monte-Carlo neutrals calculations from DEGAS, to predict the reduction of the core ionization due to the increasingly more baffled DIII–D divertors. For this calculation, we have focused on the influence of the baffle geometry; the cryopumps are not part of the calculation. Non-orthogonal grids were used to obtain the UEDGE plasma solution so that the recycling off the slanted structures could be more accurately estimated. The calculations were summarized by computing F which is defined as the ratio of the calculated core ionization current for a particular baffled divertor to the value for an open divertor. As reported previously, the calculated reduction for D-1998 is F = 3.75 for SN and F = 1.6 for DN plasma operation. For the installed D-2000 divertor, we calculate F = 6 (SN) and 1.8 (DN). (Note that previous calculations reported F = 9 because of plans to install the baffle on the inner wall).

A comparison of experimental results with the modeling shows that we measure ↔ (calculate with the model) F = 2.6 ↔ (3.75) for D-1998 and F = 5 ↔ (6) for D-2000 in SN operation, demonstrating a reasonable level of predictability with the UEDGE-DEGAS modeling. Two specially- prepared similar plasmas were used for comparison, as shown in Fig. 3. These plasmas were similar with those used in the UEDGE/DEGAS model calculations, and were ELMing H–mode plasmas with the ∇B drift direction towards the active divertor plate in each case. The core ionization was calculated in each case by detailed analysis of the edge n_e and T_e profiles with a technique described in Ref. [17]. To make a direct comparison with the model prediction (which is normalized to the current at the plate), we have corrected the data for the difference in the recycling current at the divertor plate.

3.2. DIVERTOR DETACHMENT IN D-2000

UEDGE modeling and experience on other machines with baffled divertors predicted that D-2000 would detach at a significantly lower core density, which could unnecessarily complicate these initial AT scenarios. Recall that with D-1998, we observed that the plasma transitioned to the PDD state at a 20% lower density than in the baffled divertor. UEDGE modeling of D-2000 indicated that the divertor plasma easily transitioned to a lower T_e, but perhaps not a true PDD solution over a wide range of core densities. Experimentally, we have not found a significant reduction in the core density for the PDD state in D-2000. We do, however observe a more gradual lowering of the divertor T_e until the final PDD state is obtained; more detailed data will be obtained during the remainder of the 2000 campaign.

3.3. DENSITY CONTROL IN AT PLASMAS WITH D-2000 AND WITH IMPROVED DIVERTOR DIAGNOSTICS

The increased pumping of the new divertor D-2000 has been used to obtain AT target plasmas at 0.3–0.4 of the Greenwald density, as shown in Fig. 4 [18]. D-2000 provides more core particle exhaust with a second liquid-helium cooled cryopump and plenum located near the inner strike point. The pump design and operating parameters are identical to the other pumps in DIII–D. The time evolution of the exhaust I_{ex} is obtained from the product of the measured deuterium pumping speed of the upper outer (inner) system S_{out} = 30 k ls^{-1}(S_{inner} = 20 k ls^{-1}) times the measured plenum pressure (ASDEX gauge). Operation with either pump or both pumps has been demonstrated. The discharge shown in Fig. 4(b) uses both pumps to maintain an AT target plasma at 0.3 times the Greenwald density.

Also shown in Fig. 4(a) are the new diagnostics that have been installed in the upper divertor, which include an extensive Langmuir probe array, visible spectroscopy chords, a tangential TV,

a Penning gauge, and magnetic probes. While not as extensive an array as for the lower (low-δ) divertor, we are using results from more detailed measurements in the lower divertor (i.e. with divertor Thomson scattering) to study the processes in the more baffled divertor. In particular, the tangential TV can measure ratios of D_γ/D_α emissions in a single shot, and is used to determine the degree of detachment. These data indicate that the target plasmas shown in Fig. 4 are attached, even with the highly baffled divertor.

Recent experiments have shown that D-2000 has adequate exhaust for density control at the AT core densities, and the exhaust can be regulated by strike-point sweeping. Previous experiments with the other cryopumps showed that I_{ex} can be increased (decreased) by decreasing (increasing) the distance between the separatrix and the pump aperture. With D-2000, the extensive Langmuir probe array has enabled new measurements of the exhaust efficiency η_{pump}, which is defined to be the integrated incoming ion flux measured by the Langmuir probes Γ_{in} divided by the pump exhaust I_{ex}. Preliminary analysis indicates that η_{pump} is on the order of ~10%, and *does* vary with the separation between the strike point and the pump opening at these densities. We have not observed a dependence of η_{pump} on the direction of the ∇B drift. The general relationship of the exhaust with strike point location can be understood by a simple analytic model due to Maingi, et al. [19]. At a given separatrix location, the particle source at the pumping plenum depends on a geometric solid angle factor and the probability that the particle will reach the plenum before it ionizes in the divertor plasma. (For reference, it should be noted that preliminary experiments at high density, close to or above the Greenwald density, show that η_{pump} was not as sensitive to the strike point location, presumably due to the larger divertor density and recycling.)

3.4. AT SCENARIO CONTROL WITH DIVERTOR SHAPING

In addition to strike point regulation of pumping, we have developed other useful AT control parameters based on real-time shape control, including up/down heat and particle flux sharing and control of the H–mode power threshold. As presented in Ref. [20], we find that the up/down divertor heat balance is a sensitive function of the DN magnetic balance parameter drsep (the separation at the midplane of the flux surfaces corresponding to the upper and lower X-points), and balance is obtained with a slightly unbalanced magnetic configuration. While not an issue for present DIII–D operations, this is an important consideration if both divertors are to share the heat flux equally. The up/down particle balance is much less sensitive to drsep, resulting in a weaker dependence of the exhaust on drsep or the direction of the ∇B drift. This means that particle exhaust can be obtained in DN plasmas over a range in drsep of ± 2 cm, and we can use strike point control to control the particle exhaust. Several methods of controlling the H–mode threshold power have been discovered and are used in the AT scenario development. With the ∇B drift down, we find that we can raise the H–mode power threshold by magnetically unbalanc-

ing the plasma upwards (drsep = +2 cm). We can also raise the power threshold by raising the distance between the x-point and the divertor plate.

Figure 5 shows an example of an AT scenario that takes advantage of time-dependent discharge shaping for controlling the H–mode transition and the particle exhaust. In the first panel on the left, the plasma is magnetically unbalanced upward (∇B drift down) with drsep > +2 cm and the strike point away from the outer pump aperture to maintain an unpumped L–mode plasma with high internal inductance ℓ_i. The initial L–mode phase maintains a peaked density profile for effective neutral beam absorption and the desired initial q-profile. When the q-profile has reached the desired shape, drsep is decreased to nearly 0 (magnetic balance), which triggers the H–mode transition and the concomitant increase in confinement. The neutral beam power is controlled (with real-time feedback) so as to keep β_N less than the product $4 \times \ell_i$; other techniques are also used to avoid other MHD events. The strike point is then swept out towards the upper pump to maintain the density required for the ECCD injection. These phases of the scenario have been developed, and we will start injecting ECCD in the latter half of the 2000 campaign.

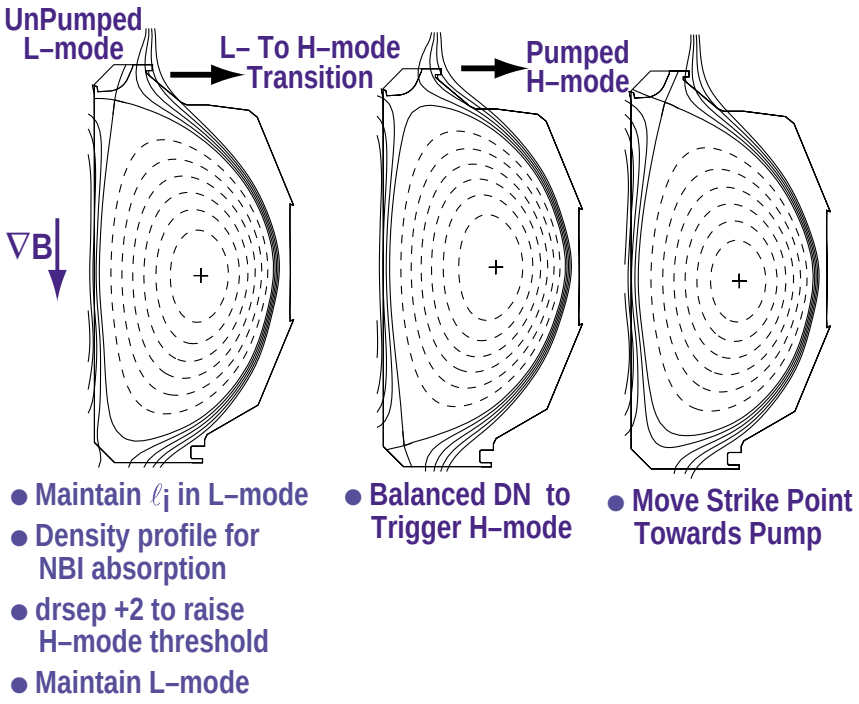

Fig. 5. One illustration of how plasma shape can control the particle exhaust and the H–mode power threshold. From left to right, the magnetic balance parameter drsep is +2 cm to raise the H–mode threshold in the beginning of the discharge to provide a peaked density profile for efficient beam penetration. The drsep is then set close to 0, magnetic balance, to trigger H–mode and increase the confinement. Shortly after this time, the strike point is swept towards the pump to maintain the target density for the ECCD portion of the discharge.

In the AT scenarios, the evolution of the q-profile depends on the plasma conductivity profile and the applied current drive; in turn the core impurity (and T_e) profiles determine the conductivity profile. The importance of this relationship is demonstrated by recent experiments on DIII–D with D-2000. As mentioned above, we have taken special care to shape the divertor tiles surrounding the inner strike point. IRTV data was obtained when the plasma was swept from a region where the tiles were not shaped (as in D-1998) to the shaped region, and we observed a dramatic decrease in the heating of the edges of the tiles. Furthermore, the core carbon impurity content was reduced for these discharges compared to previous operation with D-1998. While the operation at reduced Z_{eff} is favorable, we have had to retune the AT scenario because of the change in the core conductivity and the resulting change in the q-profile evolution.

4. RADIATIVE DIVERTOR OPERATION IN AT SCENARIOS WITH FLOW CONTROL ("PUFF AND PUMP")

Heat flux control in AT discharges will require increases in the core and divertor density from the present DIII–D regimes (with addition ECCD) and increased divertor and mantle radiation with artificially introduced impurities such as argon. In DIII–D P&P, experiments, a large deuterium gas puff with equal pumping exhaust enriches the impurities in the divertor region. In the lower divertor, experiments with trace argon achieved enrichment factors as large as 18, with smaller numbers for neon. When the injected impurity levels were increased to the point of significant radiation, both carbon and argon radiation increased both in the divertor and in a mantle around the core. The SOL plasma was also more robust and provided better shielding against impurity penetration. Preliminary trace argon P&P experiments have been carried out with D-2000 divertor, and we have seen significant exhaust of injected argon with main chamber deuterium puffing compared to divertor puffing.

Experimental data and computational models continue to point to important physics in the region of the X-point and the private flux region. Private flux flows from the outer strike point towards the inner strike point which reverse with the direction of the toroidal field have been observed in L–mode, and UEDGE modeling with drifts is making progress in understanding these flows. Mach probe and spectroscopic measurements of flows have shown complicated flow patterns near the X-point and in the SOL which are consistent with UEDGE modeling. Recombination has been observed in the private flux region. Understanding these mechanisms is necessary to optimize the impurity flow control techniques in the divertor.

5. SUMMARY

The AT scenarios highlight the close coupling between the core and divertor plasmas, and the importance of plasma shaping and impurity control. Divertors are no longer "just for heat flux reduction", but are also used for density control and to control the H–mode power threshold. The new D-2000 divertor has achieved sufficient density control for the near-term ECCD scenarios on DIII–D. Significant progress with AT modes has been made on DIII–D so that a β_N H product of 9 has been achieved for over 16 energy confinement times. An AT scenario that uses discharge shape control to optimize the q-profile and particle exhaust has been developed. We are currently injecting 2–3 MW of ECCD power to sustain the q-profile needed for these AT modes.

REFERENCES

[1] ITER Team, Nucl. Fusion **39**, 2137 (1999).
[2] B. Lipschultz, M.A. Mahdavi, G.D. Porter, *et al*., in *US Summer Workshop*, Snowmass, Colorado, 1999).
[3] S.L. Allen, N.H. Brooks, R. Bastasz, *et al*., Nucl. Fusion **39**, 2015 (1999).
[4] N. Asakura, S. Sakurai, N. Hosogane, *et al*., Nucl. Fusion **39**, 1983 (1999).
[5] AW. Leonard, M.A. Mahdavi, S.L. Allen, *et al*., Phys. Rev. Lett. **78**, 4769 (1998).
[6] T.W. Petrie, S.L. Allen, T.N. Carlstrom, *et al*., J. Nucl. Mater. **241-243**, 639 (1997).
[7] M.E. Fenstermacher, S.L. Allen, D.N. Hill, *et al*., J. Nucl. Mater. **266-269**, 348 (1999).
[8] T.H. Osborne, M.A. Mahdavi, G.R. McKee, *et al*., this conference.
[9] M.R. Wade, J.T. Hogan, R.C. Isler, *et al*., in *17th IAEA Fusion Energy Conference*, Yokahama, Japan, 1998).
[10] D.G. Whyte, W.P. West, R. Doerner, *et al*., this conference
[11] W.P. West, G.D. Porter, T.E. Evans, *et al*., this conference.
[12] G.D. Porter, T.D. Roglien, M.E. Rensink, *et al*., this conference.
[13] S. Ishida, JT-60 Team, Nucl. Fusion **39**, 1211 (1999).
[14] T.S. Taylor, K.H. Burrell, D.R. Baker, *et al*., in *17th IAEA Fusion Energy Conference*, Yokahama, Japan, 1998).
[15] JET Team, Nucl. Fusion **39**, 1227 (1999).
[16] F. Najmabadi and the ARIES Team, FED 38 (1997).
[17] G.D. Porter, S. Davies, B. LaBombard, *et al*., J. Nucl. Mater. **266-269**, 917 (1999).
[18] M.A. Mahdavi, S.L. Allen, J.A. Boedo, *et al*., this conference.
[19] R. Maingi, J.G. Watkins, M.A. Mahdavi, *et al*., Nucl. Fusion **39**, 1187 (1999).
[20] T.W. Petrie, S.L. Allen, M.E. Fenstermacher, *et al*., this conference.

ACKNOWLEDGMENTS

Work supported by U.S. Department of Energy under Contracts DE-AC03-89ER51114, DE-AC05-96OR22464, W-7405-ENG-48, DE-AC04-94AL85000, and Grant DE-FG03-95ER54294.